2008 IEEE International Conference on
Robotics and Automation
Pasadena, CA, USA, May 19-23, 2008

Dexterous Hyper Plate Inspired by Pizza Manipulation

Mitsuru Higashimori, Keisuke Utsumi, and Makoto Kaneko

Abstract— **This paper discusses a dexterous hyper plate inspired by pizza manipulation. We first discuss the necessary combinations of active degrees of freedom of the plate for manipulating an object to arbitrary position and orientation on the plate, under the gravity. While there are nine patterns for choosing two active degrees of freedom of the plate, we show one of them can satisfy a sufficient condition for manipulating the object with the weakest coupling among object's motions and eventually leads to a simple manipulation scheme. A couple of experiments are shown to confirm the basic idea.**

I. Introduction

Motivation: Fig.1 shows that a master of Italian pizza restaurant is manipulating a pizza in an oven by grasping a bar whose end is attached with a plate. He can dexterously manipulate both position and orientation of pizza on the plate, by using inertia force, frictional force, and gravitational force, respectively. For manipulating a pizza on the plate, he is mainly using two active motions for the plate; one is for pushing and pulling motion along the longitudinal axis of the bar, and the other is for rotating motion around the longitudinal axis of the bar. The practical availability of this manipulation tool has been proven by its continuous use in the long history for pizza handling. We are very much interested in analyzing the advantage of this manipulation scheme including two active motions and in developing a dexterous hyper plate inspired by the pizza manipulation.

Goal of Paper: Suppose that an object is manipulated to arbitrary position and orientation on the plate under the gravity. How many active degrees of freedom (DOFs) are necessary and sufficient? In case that there are many combinations to satisfy the requirements, which combination is most appropriate from the viewpoint of simple manipulation scheme? Is the most appropriate one similar to that of the pizza manipulation? Can the developed hyper plate work dexterous enough to ensure that the considerations are valid? The goal of the paper is to answer these questions.

Main Results: We first discuss the necessary combinations of active DOFs of the plate for manipulating the object to arbitrary position and orientation. While there are nine patterns for choosing two active DOFs of the plate, six of them enable us to produce two translational object's motions as well as one rotational motion on the plate. We further show that one of six patterns can satisfy a sufficient condition with the weakest coupling among DOFs of the object's motion and eventually lead to a simple manipulation scheme. We show that one of them is a similar arrangement of active DOFs of the plate to that of the pizza manipulation. By applying this arrangement of active DOFs to the plate, we design and develop a dexterous hyper plate system with a high-speed vision, as shown in Fig.2. We show a couple of experiments for manipulation which is far beyond human capability.

Fig. 1. Manipulating a pizza by human

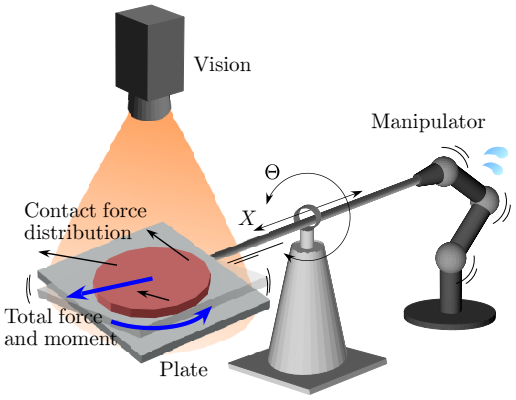

Fig. 2. Hyper plate system with two active DOFs of X and Θ

Organization of Paper: This paper is organized as follows: In Section II, we review related works. In Section III, we show the analytical model and the problem formulation. In Section IV, we discuss the necessary condition for arrangement of active DOFs of the plate to manipulate the object. In Section V, we discuss a sufficient condition and show that one of the best arrangements of active DOFs is similar to that of the pizza manipulation. In Section VI, we show the experimental results after explaining the developed hyper plate system. In Section VII, we conclude the paper.

II. Related Works

With the increase of both sensing and actuation speed, it has become possible to chase or manipulate a moving object

This work was supported by SORST of JST.

M. Higashimori and M. Kaneko are with Department of Mechanical Engineering, Osaka University, 2-1 Yamadaoka, Suita, 565-0871, Japan {higashi,mk}@mech.eng.osaka-u.ac.jp

K. Utsumi is with Hiroshima University, Higashi-Hiroshima, Japan.

[1]–[6]. Dynamic manipulation can be separated into two groups in terms of the number of fingers; one is a robot with more than two fingers, and the other is just a single plate. Kaneko *et al.* have developed a two-fingered robot that can achieve the acceleration of 100[G]. Namiki *et al.* have developed a three-fingered robot hand by implementing a powerful actuator for each joint and achieved various experiments concerning with dynamic catching. Reznik and Canny [7] have developed the Universal Planar Manipulator (UPM) base on a single horizontally-vibrating plate with three DOFs. They have demonstrated that multiple objects were simultaneously moved toward target directions. Vose *et al.* [8] have discussed a sensorless control method for an object on a rigid plate with a vibration around an arbitrary axis and shown a basic experimental result by using one DOF vibration generated by a speaker. However, as far as we know, there are no works inspired by the pizza manipulation.

III. Problem Formulation

Consider a plate and an object as shown in Fig.3. For simplifying the analysis, we set the following assumptions:

1: Both the plate and the object are rigid.
2: The object has a uniform mass distribution and a negligible thickness.
3: The plate is large enough not to drop the object.
4: The area contact between the plate and the object is maintained.
5: The friction coefficient based on Coulomb's law is given by μ between the plate and the object, where static friction and dynamic one are not distinguished.
6: The position and the orientation of both the plate and the object can be observed.

The meanings of symbols in Fig.3 are as follows:

Σ_R: The reference coordinate system. The x_R-y_R plane is horizontal.
Σ_m: The coordinate system fixed at the plate. The z_m-axis is perpendicular to the plate.
Σ_B: The coordinate system fixed at the center of mass of the object. The z_B-axis is perpendicular to the contact plane.
${}^m x_B, {}^m y_B$: The position of Σ_B with respect to Σ_m.
${}^m \theta_B$: The orientation of Σ_B with respect to Σ_m.
m_B: The mass of the object.
A_B: The contact area between the object and the plate.
g: The gravitational acceleration.

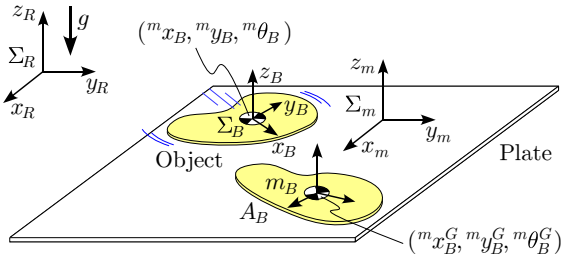

Fig. 3. Model for analysis

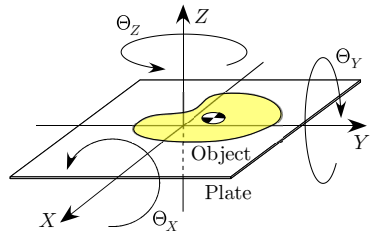

Fig. 4. A plate with six DOFs

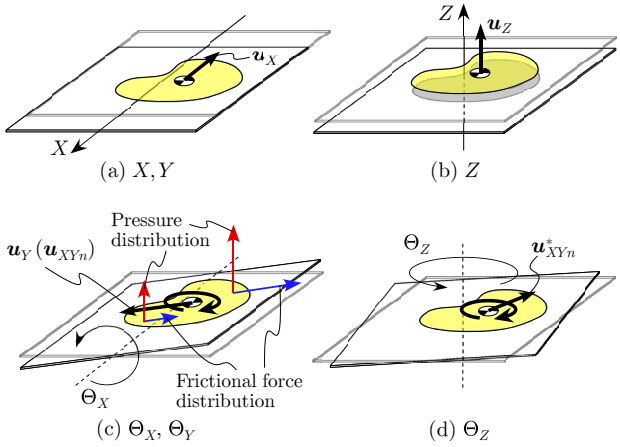

Fig. 5. Object's motion generated by a plate with one ADOF

Under the above preparation, we treat the following problem: By utilizing plate motions with as small number of active DOFs as possible, we control the position and the orientation of the object $({}^m x_B, {}^m y_B, {}^m \theta_B)$ with respect to the plate, and we transport the object from the initial set of position and orientation given by $({}^m x_B^S, {}^m y_B^S, {}^m \theta_B^S)$ to the goal set of position and orientation given by $({}^m x_B^G, {}^m y_B^G, {}^m \theta_B^G)$.

IV. Necessary Condition

Fig.4 shows a horizontal plate and an object, where X, Y, and Z denote three axes for translational DOFs of the plate perpendicular to each other, respectively, while Θ_X, Θ_Y, and Θ_Z denote the rotational DOFs around X, Y, and Z, respectively, where Z corresponds to the vertical direction. Let us now consider how many active DOFs (ADOFs) are necessary for generating three DOFs of object's motion on the plate, namely two DOFs of translational motion and one DOF of rotational one around the center of mass.

Plate with one ADOF: Suppse that the plate has only one ADOF among the above six DOFs, while the other five DOFs are fixed with respect to the reference coordinate system Σ_R. In this case, we can classify the relationship between the plate's motion and the resultant object's one into four patterns as shown in Fig.5(a)–(d), respectively. Fig.5(a) shows the pattern where the plate has the X- or the Y-deirctional ADOF, while the case of X is shown in the figure. In this case, one DOF of translational object's motion can be generated when the inertial force applied to the object is greater than the contact friction. Let the total force and moment vector shown by $\boldsymbol{u}_X \triangleq (f_X, 0, 0, 0, 0, 0)^T$ (or $\boldsymbol{u}_Y \triangleq (0, f_Y, 0, 0, 0, 0)^T$) express such a force whose

TABLE I

OBJECT'S MOTION GENERATED BY A PLATE WITH TWO ADOFS

Figure	Comb. of ADOFs	X	Y	Z	Θ_X	Θ_Y	Θ_Z	by Comb.	Three DOFs	Two decoupled DOFs
Fig.6(a)	X, Y	$\boldsymbol{u}_X$	$\boldsymbol{u}_Y$	-	-	-	-	$\boldsymbol{u}_{XY}$	×	×
Fig.6(b)	X, Z	$\boldsymbol{u}_X$	-	$\boldsymbol{u}_Z$	-	-	-	$\boldsymbol{u}_{XZ}$	×	×
	Y, Z	-	$\boldsymbol{u}_Y$	$\boldsymbol{u}_Z$	-	-	-	$\boldsymbol{u}_{YZ}$		
Fig.6(c)	X, Θ_X	$\boldsymbol{u}_X$	-	-	$\boldsymbol{u}_Y(\boldsymbol{u}_{XYn})$	-	-	$\boldsymbol{u}_{XY}(\boldsymbol{u}_{XYn})$	○	○
	Y, Θ_Y	-	$\boldsymbol{u}_Y$	-	-	$\boldsymbol{u}_X(\boldsymbol{u}_{XYn})$	-	$\boldsymbol{u}_{XY}(\boldsymbol{u}_{XYn})$		
Fig.6(d)	X, Θ_Y	$\boldsymbol{u}_X$	-	-	-	$\boldsymbol{u}_X(\boldsymbol{u}_{XYn})$	-	$\boldsymbol{u}_X(\boldsymbol{u}_{XYn})$	○	×
	Y, Θ_X	-	$\boldsymbol{u}_Y$	-	$\boldsymbol{u}_Y(\boldsymbol{u}_{XYn})$	-	-	$\boldsymbol{u}_Y(\boldsymbol{u}_{XYn})$		
Fig.6(e)	X, Θ_Z	$\boldsymbol{u}_X$	-	-	-	-	$\boldsymbol{u}^*_{XYn}$	$\boldsymbol{u}_{XYn}$	○	×
	Y, Θ_Z	-	$\boldsymbol{u}_Y$	-	-	-	$\boldsymbol{u}^*_{XYn}$	$\boldsymbol{u}_{XYn}$		
Fig.6(f)	Z, Θ_X	-	-	$\boldsymbol{u}_Z$	$\boldsymbol{u}_Y(\boldsymbol{u}_{XYn})$	-	-	$\boldsymbol{u}_Y(\boldsymbol{u}_{XYZn})$	○	×
	Z, Θ_Y	-	-	$\boldsymbol{u}_Z$	-	$\boldsymbol{u}_X(\boldsymbol{u}_{XYn})$	-	$\boldsymbol{u}_X(\boldsymbol{u}_{XYZn})$		
Fig.6(g)	Z, Θ_Z	-	-	$\boldsymbol{u}_Z$	-	-	$\boldsymbol{u}^*_{XYn}$	$\boldsymbol{u}^*_{XYZn}$	×	×
Fig.6(h)	Θ_X, Θ_Y	-	-	-	$\boldsymbol{u}_Y(\boldsymbol{u}_{XYn})$	$\boldsymbol{u}_X(\boldsymbol{u}_{XYn})$	-	$\boldsymbol{u}_{XY}(\boldsymbol{u}_{XYn})$	○	○
Fig.6(i)	Θ_X, Θ_Z	-	-	-	$\boldsymbol{u}_Y(\boldsymbol{u}_{XYn})$	-	$\boldsymbol{u}^*_{XYn}$	$\boldsymbol{u}_{XYn}$	○	×
	Θ_Y, Θ_Z	-	-	-	-	$\boldsymbol{u}_X(\boldsymbol{u}_{XYn})$	$\boldsymbol{u}^*_{XYn}$	$\boldsymbol{u}_{XYn}$		

direction is constrained. Fig.5(b) shows the pattern where the plate has the Z-deirctional ADOF. In this case, $\boldsymbol{u}_Z \triangleq (0, 0, f_Z, 0, 0, 0)^T$ pushing the object up from the plate, can be generated. Fig.5(c) shows the pattern where the plate has the Θ_X- or Θ_Y-directional ADOF. In this case, if the plate is rotated with slow enough to neglect any dynamic effects, the object receives the translational force of $\boldsymbol{u}_Y$ (or $\boldsymbol{u}_X$) only by the gravitational effect. On the other hand, if the plate is rotated with a high speed, the slope of the pressure distribution on the object is large enough to ensure that the frictional force produces a moment around the center of mass of the object [9]. This moment is coupled with f_X and f_Y, so the total force and moment are given by $\boldsymbol{u}_{XYn} \triangleq (f_X, f_Y, 0, 0, 0, n_Z)^T$, where the subscript n of $\boldsymbol{u}$ denotes n_Z. We would note that n_X and n_Y never be generated by Assumption 4. Thus, the Θ_X-directional ADOF produces the decoupled force $\boldsymbol{u}_Y$ and the coupled force and moment $\boldsymbol{u}_{XYn}$. The later one is described within () in the figures. We would once note that this pattern can produce three object's motions while they are strongly coupled each other. Fig.5(d) shows the motion pattern produced by the Θ_Z-directional ADOF. In this case, the moment of n_Z is generated by the inertial effect with respect to the angular acceleration of the plate. In addition to this, f_X and f_Y are generally generated by the centrifugal force. However, such a translational force can be generated only under that the center of mass of the object is away from the Z-axis and it has no reversibility. We refer that such a force is expressed by $\boldsymbol{u}^*_{XYn}$ where we segregate it from the vector shown in Fig.5(c). From the above discussions, the plate with one ADOF has a potential capability to generate three DOFs of the object's motion, when we provide the Θ_X- or the Θ_Y-directional ADOF for the plate, as shown in Fig.5(c). This is the minimum ADOF pattern satisfying our requirement. Therefore, the ADOF pattern as shown in Fig.5(c) can satisfy the necessary condition.

Plate with two ADOFs: Now, let us consider that the plate has two ADOFs. In this case, there are totally fifteen combinations of ADOFs as shown in Table I. We can classify them into nine patterns as shown in Fig.6(a)–(i). Table I

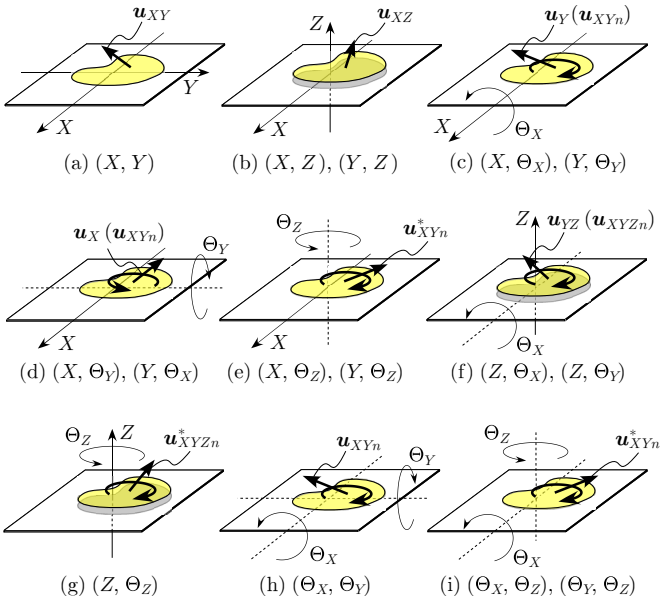

Fig. 6. Object's motion generated by a plate with two ADOFs

shows the total force and moment vector generated by using each one ADOF independently among two ADOFs and the vector by using both two ADOFs simultaneously. When one ADOF is utilized independently, the total force and moment vectors as shown in Fig.5 are applied. In the case where two ADOFs are combined, total force and moment vectors for the object include coupling components as shown in Fig.6(a)–(i). In the case as shown in Fig.6(e) and (i), although Θ_Z generates $\boldsymbol{u}^*_{XYn}$, the plate with two ADOFs has a reversibility, since another ADOF can generate a translational force toward the Z-axis. As shown in Table I, the patterns of two ADOFs for the plate with a potential capability to generate the total force and moment including f_X, f_Y, and n_Z are six as shown in Fig.6(c)–(f), (h), and (i). These can satisfy the necessary condition.

V. SUFFICIENT CONDITION

We now discuss a sufficient condition where we examine whether there exists a motion planning to ensure that the

object can be manipulated to a goal set of position and orientation or not. While two of nine patterns can generate two decoupled DOFs of the object's motion which is good for a simple manipulation scheme, we would note that one of them is similar to the pizza manipulation in terms of ADOFs. This means that the arrangement of ADOFs of the pizza manipulation has a great advantage from the viewpoint of preparing a simple manipulation scheme. We would now note that the number of the input parameters is one or two of ADOFs of the plate and that of the output parameters is three of the position and the orientation of the object, namely, the dynamic system is under nonholonomic constraints.

A. Relationship between Pizza Manipulation and Nine Patterns of two ADOFs

While there are totally nine patterns of two ADOFs of the plate as shown in Fig.6, there are six patterns satisfying the necessary condition where the plate can generate three DOFs of the object's motion. Since a translational motion and a rotational one given to the object are complicatedly coupling in general, we often have to prepare a complex motion planning for achieving both desired position and orientation simultaneously. However, when two decoupled DOFs of the object's motion can be generated, we can consider a simple motion planning. For example, we first achieve the desired position for the coupled axis, and then achieve the desired positions for two decoupled axes one by one. The patterns of ADOFs of the plate which can generate two decoupled DOFs of the object's motion are $(\xi, \Theta_\xi : \xi = X \text{ or } Y)$ and (Θ_X, Θ_Y) as shown in Fig.6(c) and (h), respectively, which are with the weakest coupling among DOFs of the object's motion. Now, it is interesting to note that (ξ, Θ_ξ) as shown in Fig.6(c) is a similar arrangement of ADOFs to that of the pizza manipulation. By focusing on the analogy with the pizza manipulation, in this work, we pick up (ξ, Θ_ξ). Suppose that a plate is attached at the tip of a bar as shown in Fig.7(a) and (b). Σ_m is fixed at the connecting point between the plate and the bar, where the x_m- and the z_m-axes coincide with the longitudinal direction of the bar and the perpendicular direction to the plate, respectively. X and Θ express the translational displacement along the x_m-axis and the rotational angle around the x_m-axis, respectively, where $\Theta = 0$ when the plate is horizontal. In order to confirm the sufficiency, we consider whether there exists a manipulation scheme for achieving a goal set of position and orientation of the object or not. In the next section, we first discuss plate's motion for generating object's motions for the x_m- and the y_m-directions and the rotation, respectively.

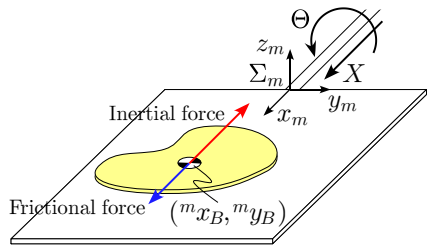

(a) The x_m-direction

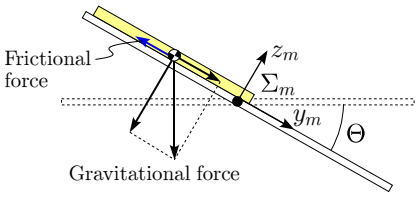

(b) The y_m-direction

Fig. 7. Translational motions of object

B. Translational Motions of Object

Suppose that the plate and the object are stationary ($X = 0, \Theta = 0$). The X directional motion of the plate produces the inertial force of $-m_B\ddot{X}$ to the object as shown in Fig.7(a). With the consideration of the maximum frictional force of $\mu m_B g$, the plate motion for generating the object's acceleration of ${}^m\ddot{x}_B$ is given by

$$|\ddot{X}| > \mu g. \tag{1}$$

Since the translational axis of plate is perpendicular to the y_m-axis, the x_m-directional motion of the object is completely decoupled with both the y_m-directional and the rotational motions. For generating continuous motions toward one direction, we have to give the plate with different magnitudes of $\ddot{X}$ between the positive and the negative directions. In the same way, suppose that the plate and the object are stationary ($X = 0, \Theta = 0$). For generating the object's acceleration of ${}^m\ddot{y}_B$, we can utilize the gravitational force, as shown in Fig.7(b). With the y_m-directional component of gravity of $-m_B g \sin\Theta$ and the maximum frictional force of $\mu m_B g \cos\Theta$, the angle of plate Θ is given by

$$|\Theta| > \tan^{-1}\mu. \tag{2}$$

Since the rotational axis of plate corresponds to the x_m-axis, the y_m-directional motion of the object can be generated with being completely decoupled with both the x_m-directional and the rotational motions. These discussions explain that there exists a manipulation scheme for controlling two DOFs of translational motion.

C. Rotational Motion of Object

As shown in Fig.8(a), suppose that the object starts to slip and moves along the x_m-direction by the motion of plate with $\ddot{X}$ based on (1). In this case, as the pressure distribution on the object is uniform, the frictional force distribution is also uniform, as shown in Fig.8(a), where we simply draw the frictional distribution on the line segment which passes through the center of mass of object and runs parallel with the y_m-axis. Let us now consider the case when the plate motion of $\ddot{\Theta}$ is added as shown in Fig.8(b). In such a case, the pressure distribution on the object results in a slope by the inertial force generated by $\ddot{\Theta}$. The pressure applied to a small area dA around an arbitrary point of the object denoted by $({}^m x_r, {}^m y_r)$ is given by

$$p({}^m y_r) = \frac{m_B}{A_B}(g + {}^m y_r \ddot{\Theta}). \tag{3}$$

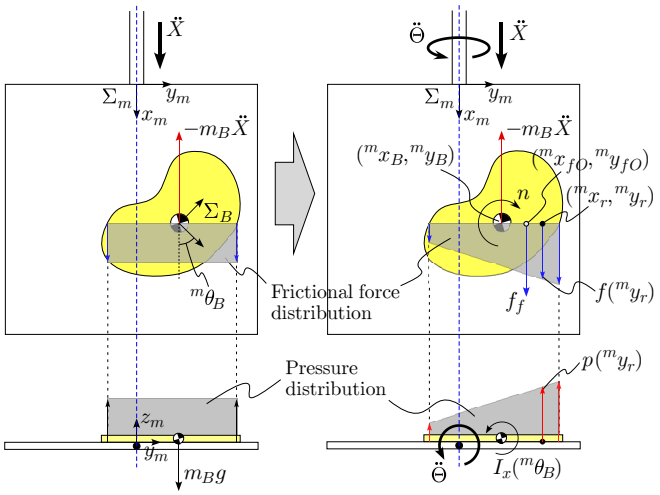

(a) Plate motion of X (b) Plate motions of X and Θ

Fig. 8. Rotational motion of object

As shown in (3), the pressure distribution on the object is the function of ${}^my_r$. From (3), the total moment applied around the center of mass of the object can be expressed by

$$n = -\frac{{}^m\dot{x}_B}{|{}^m\dot{x}_B|}\mu\int_{A_B}({}^my_r - {}^my_B)\cdot p({}^my_r)dA, \quad (4)$$

$$= -\frac{{}^m\dot{x}_B}{|{}^m\dot{x}_B|}\mu(g + {}^my_B\ddot{\Theta})\int_{m_B}({}^my_r - {}^my_B)dm - \frac{{}^m\dot{x}_B}{|{}^m\dot{x}_B|}\mu\ddot{\Theta}\int_{m_B}({}^my_r - {}^my_B)^2dm, \quad (5)$$

where $n > 0$ and $n < 0$ coincide with the moments of the clockwise and the counter clockwise directions, respectively. Since the first term in (5) is always zero based on the definition of the center of mass, we obtain

$$n = -\frac{{}^m\dot{x}_B}{|{}^m\dot{x}_B|}\mu I_x({}^m\theta_B)\ddot{\Theta}, \quad (6)$$

where

$$I_x({}^m\theta_B) \triangleq \int_{m_B}({}^my_r - {}^my_B)^2dm$$

is corresponding to the moment of inertia around the axis which passes through the center of mass of the object and runs parallel with the x_m-axis, when the orientation of the object is given by ${}^m\theta_B$. Therefore, (6) means that the moment applied to the object around the z_B-axis depends upon the moment of inertia around the axis perpendicular to the z_B-axis. From (6), we would also note that a general object with the moment of inertia of $I_x({}^m\theta_B) > 0$ ($0 \leq {}^m\theta_B \leq \pi$) produce a moment of $|n| \neq 0$, by giving a plate's motion of $|\ddot{\Theta}| > 0$.[1] On the other hand, the total frictional force applied to the object is given by

$$f_f = -\frac{{}^m\dot{x}_B}{|{}^m\dot{x}_B|}\mu\int_{A_B}p({}^my_r)dA, \quad (7)$$

$$= -\frac{{}^m\dot{x}_B}{|{}^m\dot{x}_B|}\mu m_B(g + {}^my_B\ddot{\Theta}). \quad (8)$$

[1]There is singular posture of object. For extreme example, suppose the case where a stick with negligible width is on the plate with parallel to the x_m-axis. Since $I_x({}^m\theta_B) \approx 0$, it is diffuicult to rotate the stick.

From (6) and (8), with the introduction of the center of friction [9] of $({}^mx_{fO} = {}^mx_B, {}^my_{fO})$, we obtain

$${}^my_{fO} - {}^my_B = \frac{n}{f_f}, \quad (9)$$

$$= \frac{I_x({}^m\theta_B)\ddot{\Theta}}{m_B(g + {}^my_B\ddot{\Theta})}. \quad (10)$$

Now let us recall Assumption 4 where the center of mass of object never be taken off from the plate. This assumption is expressed by

$$g + {}^my_B\ddot{\Theta} > 0. \quad (11)$$

From (10) and (11), ${}^my_{fO} - {}^my_B > 0$ is always guaranteed when $\ddot{\Theta} > 0$. In addition to this, when the translational motion of plate is given by $\ddot{X} > 0$ as shown in Fig.8(b), $n > 0$ is satisfied in (6) and, as a result, the object rotates for the clockwise direction. By taking into account that the center of mass of the object $({}^mx_B, {}^my_B)$ exists on the line where $-m_B\ddot{X} < 0$, the above discussions correspond to that in [9] where the object rotates for the clockwise direction when ${}^my_{fO} - {}^my_B > 0$. In the same way, when $\ddot{X} > 0$ and $\ddot{\Theta} < 0$, ${}^my_{fO} - {}^my_B < 0$ and $n < 0$ are satisfied in (10) and (6), respectively. As a result, the object rotates for the counter clockwise direction. The above discussions lead to the condition of the plate's motion for generating a rotational motion of the object is given by

$$(|\ddot{X}| > \mu g) \cap (|\ddot{\Theta}| > 0), \quad (12)$$

where $\ddot{X}\ddot{\Theta} > 0$ and $\ddot{X}\ddot{\Theta} < 0$ generate the moments for the clockwise direction ($n > 0$) and for the counter clockwise one ($n < 0$), respectively. We would now note that the rotational motion of the object is always coupled with both the x_m- and the y_m-directional translational motions, since the plate's motions of both X and Θ are utilized. These discussions explain that the rotational motion of the object is also controllable, while it is coupled with other motions.

D. For Achieving Goal set of Position and Orientation

Based on (1), (2), and (12), we can generate small object's motions by giving the plate motions with

$$(|\ddot{X}| = \mu g + \varepsilon_1) \cap (\Theta = 0), \quad (13)$$

$$(|\Theta| = \tan^{-1}\mu + \varepsilon_2) \cap (X = 0), \quad (14)$$

$$(|\ddot{X}| = \mu g + \varepsilon_3) \cap (|\ddot{\Theta}| = \varepsilon_4), \quad (15)$$

for the x_m-direction, the y_m-direction, and the rotation, respectively, where ε_1–ε_4 are small positive values, respectively. We would note that the rotational motion is coupled with both the translational motions, while the x_m- and the y_m-directional motions can be independently generated. Generally, it is not guaranteed that the position of the object after the rotation corresponds to that before the rotation. To cope with this issue, we first achieve the desired orientation of the object by the rotational motion as shown in Fig.9(a), and we then achieve the desired x_m- (or y_m-) directional position and the desired y_m- (or x_m-) directional position one

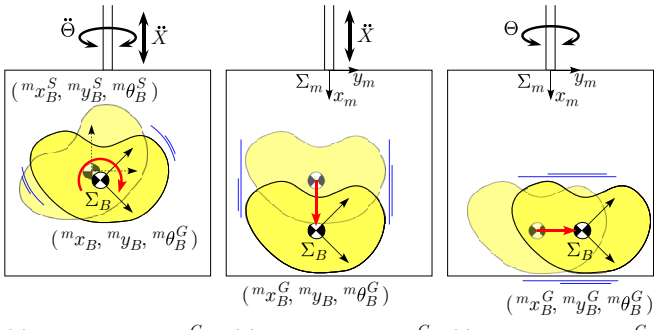

(a) Step 1: ${}^m\theta_B \rightarrow {}^m\theta_B^G$ (b) Step 2: ${}^m x_B \rightarrow {}^m x_B^G$ (c) Step 3: ${}^m y_B \rightarrow {}^m y_B^G$

Fig. 9. A manipulation scheme for achieving a goal set position and orientation

by one as shown in Fig.9(b) and (c), respectively. In such a way, it is guaranteed that the object finally reaches to an arbitrary goal set of position and orientation $({}^m x_B^G, {}^m y_B^G, {}^m\theta_B^G)$. Namely, by repeating small motions based on (13)–(15), the position and the orientation of object can be converged to the desired values under no disturbance. These discussions guarantee the sufficiency for manipulating the object by using the ADOF pattern similar to that of the pizza manipulation.

VI. Experiments

A. Experimental System

Fig.10 shows an overview of the experimental system. A plate attached at the tip of a manipulator generates the translational and the rotational motions of an object. A vision system observes the object put on the plate, and the position and the orientation of the object are utilized as feedback signals for moving the manipulator. Fig.11 shows the dexterous hyper plate and the object.[2] The dexterous hyper plate poses three active joints and one free joint, where an AC servo motor for driving each joint is implemented at each active joint. By the rotations of the 1st and the 2nd joints, the plate fixed at the tip of the bar moves along the longitudinal axis of the bar (the translational ADOF of X). By the rotation of the 4th joint, the plate rotates around the

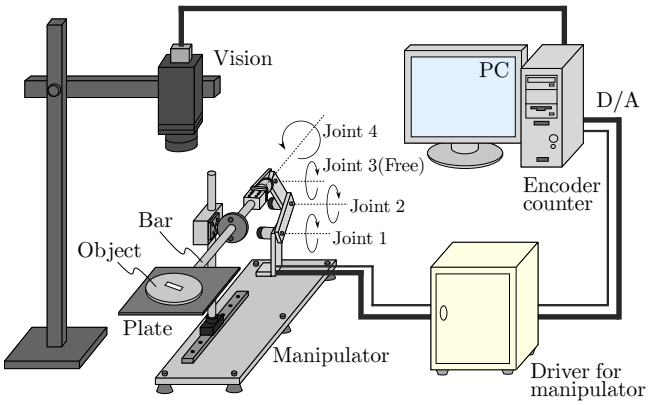

Fig. 10. Experimental system

[2]The video attachment media file for this paper shows experiments in short version. Full version can be seen in our web site:
http://www-hh.mech.eng.osaka-u.ac.jp/robotics/pizzae.html

longitudinal axis of the bar (the rotational ADOF of Θ). We would note that the plate has actually three ADOFs, while only two ADOFs of them are utilized in experiments. The plate has the size of 100[mm] $\times$ 100[mm], and the position and the orientation of the plate (X and Θ) are measured by the encoders integrated in the motors. By a bearing supporting the bar, the gravitational load applied to the joints is supported. The circular object is with the mass of $m_B = 48$[g], the radius of $r_B = 34$[mm], the moment inertia around the z_B-axis of $I_z = 28 \times 10^3$[kg·mm^2], the moment inertia around the axis perpendicular to the z_B-axis of $I_x({}^m\theta_B) = 14 \times 10^3$[kg·mm^2] $(0 \leq {}^m\theta_B \leq \pi)$, respectively. We would note that the discussion in Section V can be applied without losing generalization, while we here use a particular shape of object such as circle. The friction coefficient between the plate and the object is given by $\mu = 0.6$. We intentionally attach a rectangular shaped white marker to the center of the object so that the vision can recognize both the position and the orientation of the object.

B. Basic Motions

Fig.12 shows a series of photos where the x_m-directional motion is given to the object. Fig.13(a), (b), and (c) show the displacements of X, Θ, and ${}^m x_B$ with respect to time, respectively, where we give X a sinusoidal wave trajectory and reduce its amplitude as the object closes to the desired position of ${}^m x_B^G = 70.0$[mm]. By the operation during 1.4[s], the object moves from the initial position of ${}^m x_B^S = 25.1$[mm] to ${}^m x_B = 70.5$[mm]. Fig.14 shows a series of photos where the y_m-directional motion is given to the object. Fig.15(a), (b), and (c) show the displacements of X, Θ, and ${}^m y_B$ with respect to time, respectively, where we give Θ a sinusoidal wave trajectory and reduce its amplitude as the object closes to the desired position of ${}^m y_B^G = 20.0$[mm]. By the operation during 1.0[s], the object moves from the initial position of ${}^m y_B^S = -30.1$[mm] to ${}^m y_B = 20.9$[mm]. We would note that the stability and the robustness of the feedback system for the desired position and orientation of the object are out of discussion in this paper. Fig.16 shows a series of photos where a rotational motion is given to the object. From Fig.16(b)–(d), we can see that the object

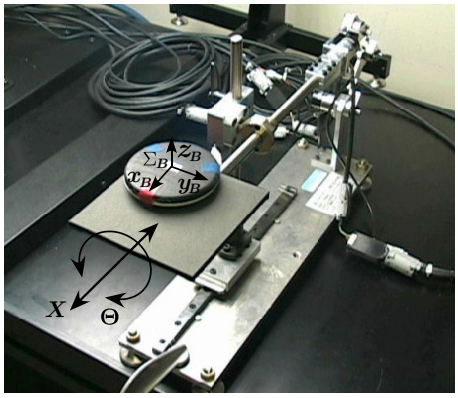

Fig. 11. An object and the dexterous hyper plate with two ADOFs

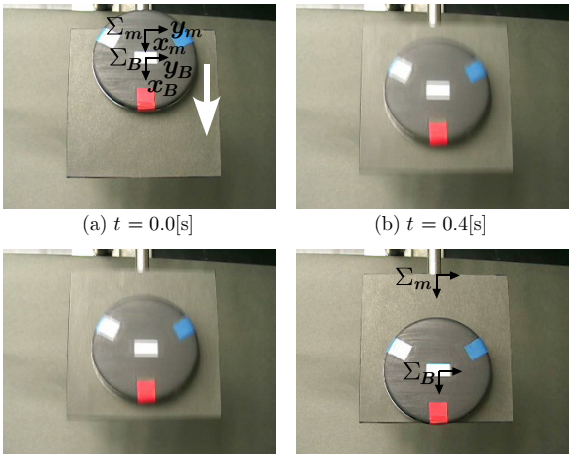

(a) $t = 0.0$[s] (b) $t = 0.4$[s]

(c) $t = 0.8$[s] (d) $t = 1.5$[s]

Fig. 12. A series of photos during the x_m-directional motion

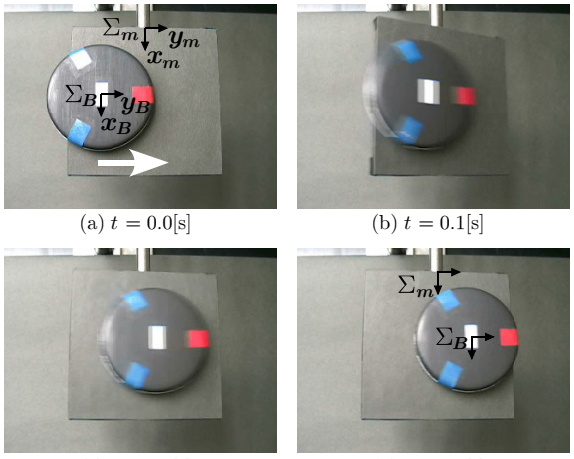

(a) $t = 0.0$[s] (b) $t = 0.1$[s]

(c) $t = 0.2$[s] (d) $t = 1.2$[s]

Fig. 14. A series of photos during the y_m-directional motion

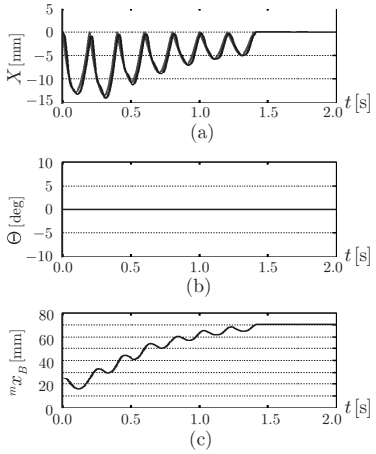

Fig. 13. Positions of the plate and the object with respect to time during the x_m-directional motion

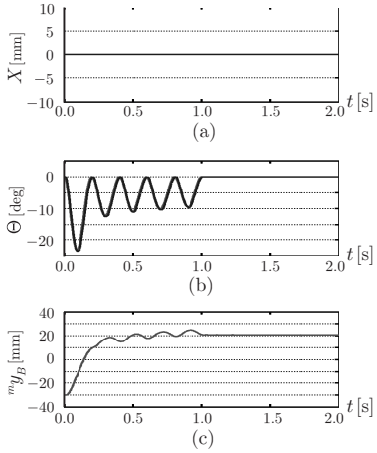

Fig. 15. Positions of the plate and the object with respect to time during the y_m-directional motion

rotates for the counter clockwise direction. Fig.19 shows the displacements of position and orientation of both the plate and the object with respect to time, where $X(t) = 8\sin 10\pi t$ and $\Theta(t) = -12\sin 10\pi t$ are given. As shown in Fig.17(c)–(e), the object rotates with the angular velocity of 27[deg/s] with coupling motions of both ${}^m x_B$ and ${}^m y_B$ around the center of the plate of $(50, 0)$[mm].

C. Goal Set of Position and Orientation

Fig.18 shows a series of photos where the plate is manipulating the object for a goal set of position and orientation, where the goal set is given by $({}^m x_B^G, {}^m y_B^G, {}^m \theta_B^G) = (70.0[\text{mm}], 20.0[\text{mm}], 120.0[\text{deg}])$ as shown by the broken line in Fig.18(a). The object is first rotated so that the goal orientation is achieved as shown in Fig.18 (a) and (b). Then, the object is moved by the x_m-directional and the y_m-directional motions as shown in Fig.18(b) and (c), respectively, and as a result, the object finally reaches the goal position as well as the goal orientation as shown in Fig.18(d). Fig.19 shows the displacements of position and orientation of both the plate and the object during the manipulation. We give the rotational, the x_m-directional, and the y_m-directional motions during $0.0 \leq t < 4.8$[s], $4.8 \leq t < 6.1$[s], and $6.1 \leq t \leq 7.0$[s], respectively. The object moves from $({}^m x_B^S, {}^m y_B^S, {}^m \theta_B^S) = (30.5[\text{mm}], -18.6[\text{mm}], 0.1[\text{deg}])$ to $({}^m x_B, {}^m y_B, {}^m \theta_B) = (68.8[\text{mm}], 18.9[\text{mm}], 121.6[\text{deg}])$.

VII. Conclusion

We discussed a dexterous hyper plate inspired by pizza manipulation. The main results are summarized as follows:

(1) We showed that while there are nine patterns for choosing two ADOFs of a plate, six of them satisfy the necessary condition to manipulate an object to an arbitrary goal set of position and orientation (Necessary condition).

(2) For the dexterous hyper plate with a similar arrangement of ADOFs to the pizza manipulation, we showed that there exists a manipulation scheme to achieve an arbitrary goal set of position and orientation of the object (Sufficient condition).

(3) We experimentally confirmed the validity of the proposed scheme by utilizing the developed dexterous hyper plate with an assistance of a vision.

The results may be applicable for dynamic parts sorting and feeding in industry. We would like to discuss a manipulation scheme for soft objects in the future.

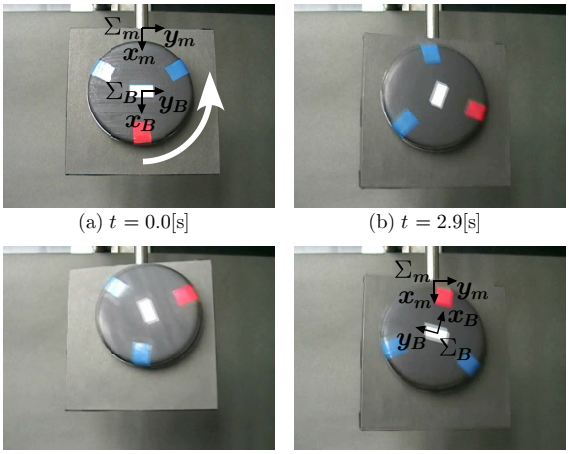

(a) $t = 0.0$[s] (b) $t = 2.9$[s]

(c) $t = 3.8$[s] (d) $t = 6.8$[s]

Fig. 16. A series of photos during a rotational motion

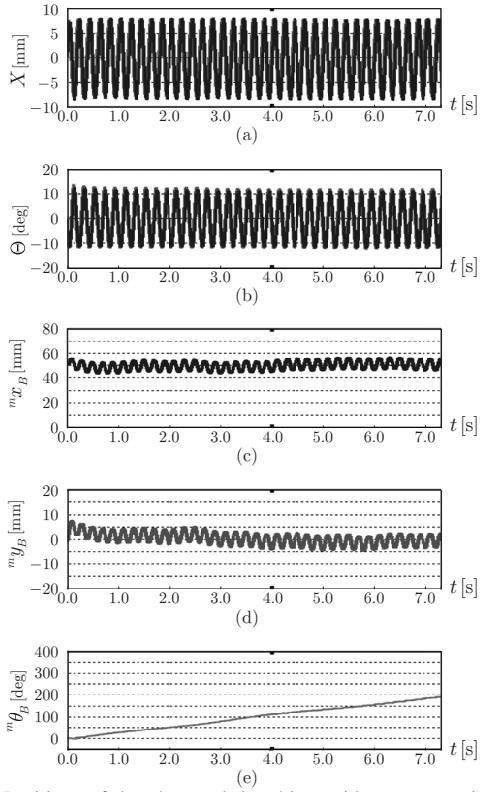

Fig. 17. Positions of the plate and the object with respect to time during a rotational motion

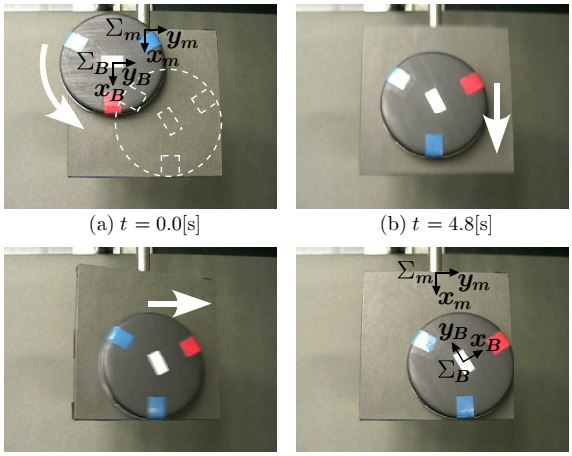

(a) $t = 0.0$[s] (b) $t = 4.8$[s]

(c) $t = 6.2$[s] (d) $t = 7.0$[s]

Fig. 18. A series of photos during a manipulation for achieving a goal set of position and orientation

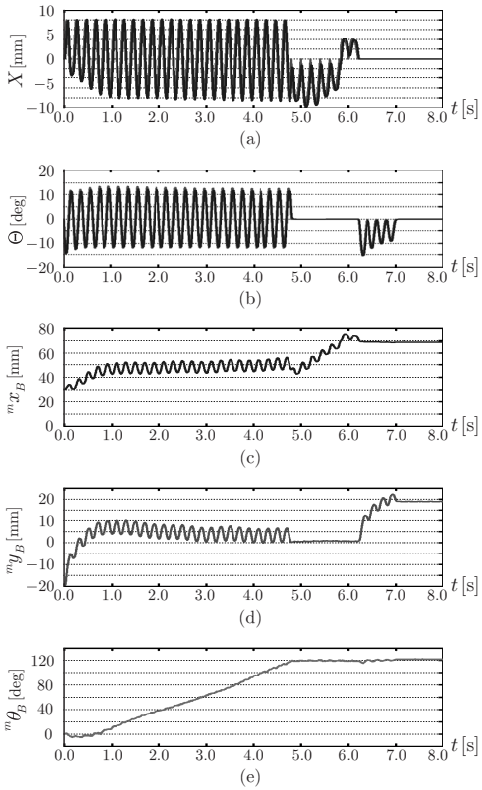

Fig. 19. Positions of the plate and the object during a manipulation for achieving a goal set of position and orientation

REFERENCES

[1] H. Arai and O. Khatib: "Experiments with Dynamic Skills," Proc. of 1994 Japan-USA Symp. on Flexible Automation, pp.81–84, 1994.

[2] K. M. Lynch, N. Shiroma, H. Arai, and K. Tanie: "The Roles of Shape and Motion in Dynamic Manipulation, The Butterfly Example," Proc. of the IEEE Int. Conf. on Robotics and Automation, pp.1958–1963, 1998.

[3] A. Amagai and K. Takase: "Implementation of Dynamic Manipulation with Visual Feedback and Its Application to Pick and Place Task," Proc. of the IEEE Int. Symp. on Assembly and Task Planning, pp.344–350, 2001.

[4] N. Furukawa, A. Namiki, S. Taku, and M. Ishikawa: "Dynamic Regrasping Using a High-speed Multifingered Hand and a High-speed Vision System," Proc. of the IEEE Int. Conf. on Robotics and Automation, pp.181–187, 2006.

[5] M. Kaneko, M. Higashimori, R. Takenaka, A. Namiki, and M. Ishikawa: "The 100G Capturing Robot -Too Fast to See-," IEEE/ASME Trans. on Mechatronics, vol.8, no.1, pp.37–44, 2003.

[6] M. Higashimori, M. Kimura, I. Ishii, and M. Kaneko: "Dynamic Capturing Strategy for a 2-D Stick-Shaped Object Based on Friction Independent Collision," IEEE Trans. on Robotics, vol.23, no.3, pp.541–552, 2007.

[7] D. Reznik and J. Canny: "C'mon Part, Do the Local Motion!," In IEEE Proc. of the IEEE Int. Conf. on Robotics and Automation, pp.2235–2242, 2001.

[8] T. Vose, P. Umbanhowar, and K. M. Lynch: "Vibration-induced frictional force fields on a rigid plate," Proc. of the IEEE Int. Conf. on Robotics and Automation, pp.660–667, 2007.

[9] M. T. Mason and J. K. Salisbury: "Robot Hands and the Mechanics of Manipulation," The MIT Press, 1985.